

# Feasibility of Constructing a Unified Positive and Negative Mass Potential

Judith Giannini

*Retired, Bellefonte, PA 16823, USA*

*Email: jag.cck@gmail.com*

*Article history:* Received 12 March 2019, Revised 23 April 2019, Accepted 25 April 2019, Published 3 May 2019.

---

**Abstract:** There is growing enthusiasm for the position that no single particle solves the puzzle of dark matter in the cosmos, a shift in perspective to include alternate ideas may offer part of the answer. Here, we advocate the (less than conventional, but not totally new) idea of negative mass as one possible contributor to the solution. We address the subject by empirically constructing a unified potential valid from the macro-gravity scales through the quantum scales that is non-symmetric between positive mass and negative mass particles. We discuss the similarities and differences between well-known potentials for traditional all-positive-mass particles, and, address the possibility that the Newtonian potential could be a first-order approximation to a sine function. Our fully unified potential ( $V_U$ ) agrees with current data-consistent potentials from the largest macro scales down to quantum scales. Unlike Newton's potential which is only a function of mass,  $V_U$  is a function of mass, and the square-root of mass which impacts the negative mass behavior. The positive mass characterization is discussed here. In the macro-scale's far field,  $V_U$  has the usual  $1/r$  decay. However, it also shows an oscillating transition between quantum-scales and macro-scales where the Casimir effect is seen. The super-massive scales also show this oscillating quantum-like behavior in the near-field region.

**Keywords:** negative mass, negative energy, alternate gravity, composite elementary particles, cosmic inflation.

---

## 1. Introduction

One of the most consuming focuses of human intellectual activity throughout history has been the need to discover the nature of our universe and its contents. In ancient times, that activity was centered prominently on the observed bodies in the heavens, along with an extensive philosophical debate on the composition of the observed matter, both astronomical and the small-scale stuff-of-everyday-life. The nature of that matter was largely unknown.

Today, most of what we know about matter in the cosmos is based on theoretical models, fed by measurements and requiring some initial assumptions [1]. Currently, the predominating consensus is the DM (dark matter) and DE (dark energy) paradigm [2], dividing the universe as: DE (identity unknown), ~73%; DM (identity unknown), ~23%; other non-luminous matter (gasses, neutrinos and super-massive black holes) and luminous matter (stars, gasses and radiation), ~4%. Numerous possible candidates have been proposed for DM [3], but to date, the search for these candidates has not been successful [4].

Simulations indicate the expected influence of DM on normal matter, leading to the strong suspicion that no single type of DM is sufficient. Several possibilities, including numerous types of particles (in addition to WIMPS and axions which have not been abandoned) and a variety of forces that act only on DM, are now on the table; and, there is growing favor with the idea that new ideas need to be considered until an answer is found [2, 5]. One direction this message leaves open is considering the dark sector – such things as parallel universes, or more unconventionally, negative mass particles (which, for the most part, until now, have been only a hypothetical concept).

The going-in assumption to most models has been that mass can only be positive. This is true, in part, because, traditionally, observed mass is the stuff we can see, and, it is unsettling to think about the opposite of what we can see. (Schiff argued in favor of assuming that all particles of matter and anti-matter have positive rest mass and positive passive gravitational mass [6, 7], a position that was later reiterated by Weinberg [8]). Also, there have been few measurements that might be interpreted as negative mass. This is starting to change, and, a paradigm shift that allows the serious consideration of negative mass as a real possibility.

The negative mass concept is not consistent with the SM as currently configured; however, it is not a unique idea in theory. Newtonian mechanics is based on a gravitational potential that is proportional to mass. There is nothing in the expression prohibiting either the active source mass ( $m_s$ ) or the passive responding test mass ( $m_t$ ) from being negative. Newton [9] reflected on the fact that we gain information about matter through observations by our senses, and, that knowledge (of “sensible bodies”) might then be applied universally to all bodies. But, he cautioned that there are bodies beyond the range of our

senses – perhaps inferring the existence of the sub-atomic world or cosmic DM that was not obvious in his time, or the real possibility of negative matter particularly DM and DE.

In his book, Jammer [10] describes some of the earliest considerations of Newton’s laws and concept of negative mass. He notes that Pearson (1885) spoke of the attractive and repulsive gravitational forces in the context of bodies in a fluid medium. Seerliger (1895) considered Newton’s law not rigorously accurate and needing supplementary terms as applied to the universe as a whole; while, A. Foppl (1897) introduced the notion of negative mass as a possible solution.

Bondi [11] stated that in Newtonian physics the law of action and reaction implies the equality of active ( $m_s$ ) and passive ( $m_t$ ) gravitational masses, but, the equality of inertial mass ( $m_i$ , that responds to non-gravitational forces) with  $m_s$  and  $m_t$  is a separate empirical fact. He noted that negative matter does not respond like ordinary (positive) matter to non-gravitational forces, producing repulsive gravitational fields. He observed that when considering relativity as a purely gravitational theory,  $m_t$  and  $m_i$  do not appear, and,  $m_s$  occurs only as an integration constant that could be either positive or negative. He went on to develop a non-singular solution to Einstein’s equations showing a repulsive force between bodies with mass densities of opposite sign.

Bonner [12] considered mechanics in a universe with negative mass and the influence of the negative mass on the Schwarzschild black hole solution. Hoyle, Burbidge and Narlikai [13] noted that allowing only positive mass results in the standard hot Big Bang model. They developed a scale-invariant form of the gravity equations that reduce to general relativity under the right conditions and leads to the creation of equal numbers of positive-mass and negative-mass particles (pairs) during creation events, providing an alternate explanation for the cosmological observations [14].

Chang [15] explored the force of negative mass and its potential relation to DM, using single-metric field equations describing repulsive interactions. In another approach, Petite and his colleagues [16] present a bimetric (Janus) model of the universe. Their theoretically model, based on Einstein’s equations, considers the interaction of positive and negative masses where the two types of matter have different light speed. Their twin-universe system of coupled equations shows like-mass-types attracting and unlike-mass-types repelling, and includes both positive-energy photons and negative-energy photons.

In a slightly different vein, FRACEP (the Fractal Rings and Composite Elementary Particles model) [17] heuristically develops composite versions of the Standard Model (SM) elementary particles and anti-particles (the “Bright Universe”) having mostly positive mass; but it also includes an additional set of dark particles and dark anti-particles (the “Dark Universe”) having mostly negative mass. The FRACEP mass types interact like the Petit-model masses, but unlike the Petite model, FRACEP

considers the mixed-mass-type internal structure of the elementary particles. The mathematical basis of this particle construction has yet to be developed.

Further, experiments are beginning to address the negative-mass question. Simone Giani [18] examined the impact of superluminal velocities on particle interactions, noting that, in such cases, the square of the particle mass needs to be negative to allow conservation of energy and momentum. His analysis of the SN1987A supernova data indicated a possible signature for superluminal neutrino bursts [19], and experiments later reconfirmed that possibility [20].

Takahashi and Asada [21] used the results of the Sloan Digital Sky Survey Quasar Lens Search to determine an upper limit on the number of negative-mass objects and Ellis wormholes. Since they are not luminous because there is no matter accretion as a result of the repulsive force, gravitational lensing was used as an observation tool to probe for these exotic objects.

Mbarek and Paranjape [22] showed that for certain conditions in an ideal fluid, there is an exact solution to Einstein's equations in a de Sitter space-time that is not asymptotically flat, indicating that any plasma of positive-negative particle pairs in the early universe would screen gravitational waves below the plasma frequency. In a related idea, Khamsehchi, et al. [23] experimentally demonstrated that with a properly engineered dispersion relation in a Bose-Einstein condensate, spin-orbital coupling exhibited behavior consistent with effective negative mass, showing that the modified dispersion resulted in soliton trains, shock waves and other non-linear effects.

Finally, the ALPHA collaboration at CERN [24] is considering the negative-mass idea from a different perspective. Big Bang theory indicates that, during the creation event, equal amounts of matter and anti-matter should have been created. They, in turn, should have annihilated each other; but, an excess of matter has survived, indicating that the laws of nature, as we understand them, do not apply equally to matter and anti-matter. The ALPHA collaboration is experimentally exploring that puzzle. Specifically, assuming the hydrogen atom is purely positive mass, is the anti-hydrogen atom purely positive (with opposite characteristics), or is it partly negative mass causing it to violate the expected gravitational attraction because there is a difference in the behavior of matter and anti-matter? Their initial efforts [25] created sufficiently stable anti-hydrogen, and further experiments are planned to more completely answer the question.

Because of the current uncertainty in the nature of dark cosmic-matter, we assume the possibility of both partially negative-mass and totally negative-mass particles [17], which requires a potential to describe their interaction with each other and with normal (positive-mass) particles. In the following sections, we describe the considerations for constructing a fully unified potential  $V_U$  that can address the differences between positive-mass and negative-mass particles at all scales. We then present a potential form and a comparison of the  $V_U$  with the two well recognized potentials (Newton and the neutron-

neutron scattering potential). A mathematical basis for this empirically constructed  $V_U$  has yet to be developed.

## 2. Consideration for Constructing a Unified Potential

$V_U$  is a unified potential that is intended to address Planck-length scales to the largest macro-scales of astronomical bodies. It characterizes both positive-mass sources and negative-mass sources. Focus is on the strong force and gravity as a way of defining the nature of  $V_U$ 's influence in the two regions where the characterization is well-known and accepted, empirically matching the behavior of the known.

Because the data available to develop  $V_U$  is for positive mass only, the derived potential function needed a broad-scale base in order to recognize the impact of negative mass on the potential form. To address the negative mass,  $V_U$  does not assume a simple replacement of “ $-m$ ” for “ $+m$ ” in any of the current potential forms. Instead, it uses current data at nuclear scales as an intermediate step between the smallest scales-of-interest and the largest macro-scale to provide a unified function that is extrapolated down to its smallest particles.

The well-known potential functions for the strong force (the SM neutron-neutron scattering potential) and for gravity (Newtonian potential  $V_N$ ) are different, but, they have some characteristic similarities. This leads to the conclusion that there might be a common rule applying to the quantum and the macro (gravity) scales, implying a single, multi-term function where all terms are not simultaneously significant at all scales.

The functional form obtained is proportional to the product of a sine function and a decaying exponential.  $V_U$  demonstrates an oscillating transition between the quantum and gravity scales, even showing a near-field oscillating (quantum-like) behavior at the very largest mass scales.  $V_U$ 's smallest possible  $r$  is  $3.3 \times 10^{-35}$  m. The negative mass characterization was not deliberately modeled – it automatically arises out of the unified functional form.

### 2.1. Familiar Macro-Scale Potential

Newtonian physics is based on a potential between two masses that decays monotonically with  $r$ ,

$$V_N = -Gm_1m_2 / r. \quad (1)$$

Experiments [26] show that  $V_N$  reflects nature to sub-millimeter  $r$ . For smaller  $r$ , it becomes difficult to distinguish between measurement uncertainty and possible variations in  $G$ . As  $r$  approaches zero,  $V_N$  grows infinitely large; but, it is uncertain if nature necessarily follows this rule. Further, general

relativity (GR) provides a correction  $(-3m_t(Gm_s/c)^2/r^2)$  [27] that resolves  $V_N$ 's perihelion advance inadequacy at cosmic scales.

With the appropriate assumptions, GR yields the same results as Newton's action-at-a-distance force. However, GR's effects also extend to super massive scales which Newton's expression does not adequately model. It also allows for repulsive energy which leads to accelerated expansion of the universe – an effect Newton cannot address. Neither Newton nor GR extend adequately to the sub-atomic levels. For that, the probabilistic formulation of quantum mechanics is required.

## 2.2. Familiar Quantum-Scale Potential

The nuclear force is based, to first order, on the well-known Yukawa potential  $V_Y = -g^2 e^{-br}/r$ , where the  $b = mc/\hbar$ ,  $\hbar$  is Planck's constant divided by  $2\pi$ , and  $g$  is analogous to the Newtonian gravitational constant  $G$ . To completely describe the nuclear force,  $V_Y$  is modified by several terms that model specific physical effects [28]. The form for neutron-neutron scattering is:

$$V_{Y-mod} \sim A V_Y [1 + S(r)\{1 + 3/(m r) + 3/(m r)^2\}] - \delta(m_\pi, r), \quad (2)$$

where,  $S(r)$ ,  $\delta(m_\pi, r)$  and  $A$  are empirically determined and  $m_\pi$  is the mass of the pi-meson exchange particle (one of the particles acting as the focus of the strong nuclear force). The usual range for current models is between  $\sim 0.3$  fm to  $\sim 2.5$  fm. The constant  $b$  in the exponential of  $V_Y$  varies depending on the mass of the exchange particle: for pi-meson exchange,  $b \sim 0.7082/\text{fm}$  where  $r > 0.3$  fm; for the rho and the omega exchanges,  $b \sim 4.054/\text{fm}$  where  $r < 0.3$  fm.

$V_{Y-mod}$  has an oscillating character that is exponentially damped with increasing  $r$ , converging to zero by  $\sim 10$  fm, making it inconsequential at macro distances. For  $r < 0.5$  fm, it grows exponentially becoming infinitely large as  $r$  approaches zero. Like  $V_N$ , it is not obvious that nature follows this rule.

## 2.3. Common Characteristics of Quantum- and Macro-Scale Behavior

$V_U$  reproduces  $V_N$ 's behavior at macro scales, and it agrees with the shape and magnitude of  $V_{Y-mod}$  at quantum scales. But, it also extends to the smallest scales without producing a singularity for positive mass sources. Several observations contributed to the construction of  $V_U$ . First, both  $V_N$  and  $V_{Y-mod}$ , to first order, have a  $1/r$  decay. Second,  $V_{Y-mod}$ 's damped oscillation is suggestive of a stretched spring, pegged at one end, and increasingly compressed in amplitude along its length. The damping is explicitly represented by an exponential decay function. The stretched oscillation is produced by the modification terms. This oscillatory effect is determined empirically in  $V_U$  by fitting to  $V_{Y-mod}$  using a sine function. For  $1/r$ , the sine function expansion is:  $\sin(1/r) = 1/r - (1/r)^3 (1/3!) + (1/r)^5 (1/5!) - \dots$

$(1/r)^{2n+1}$  ( $1/2n+1!$ ). This hints that the observed  $1/r$  behavior in  $V_{Y\text{-mod}}$  could be the first order approximation to a sine function. It could also explain the  $1/r$  behavior in  $V_N$  under the right conditions.

### 3. The Unified Potential ( $V_U$ )

The functional form of  $V_U$  was empirically determined based on the above considerations, and the numerical coefficients were determined by the best fit to the known potentials:

$$V_U = m_t [A_0(M) + B_0(\sqrt{M})] \sin[S(r, M) + T(r, \sqrt{M})] E_0(r, M); \quad (3a)$$

$$A_0 = 1 / (0.18 M),$$

$$B_0 = 9.2095 \times 10^{-8} \sqrt{M},$$

$$E_0 = \exp\{-2.4 r |M| / [M^2 + (m_{Gp} / m_\pi)]\}; \quad (3b)$$

$$S(r, M) = K_1 + K_f,$$

$$K_1 = -150 (\pi/180) 0.09 (r/M)^2 E_1,$$

$$E_1 = \exp[-67 (m_{Gp} / m_\pi) / |M|],$$

$$K_f = -(\pi/180) 0.000092 [M / 8 \times 10^{60}]^2 [1.496 \times 10^{26} / r]^3; \quad (3c)$$

$$T(r, \sqrt{M}) = K_2 + K_3 + K_4,$$

$$K_2 = -150 (\pi/180) (0.00006 / m_\pi) \sqrt{M} / r,$$

$$K_3 = 150 (\pi/180) E_1 / \sqrt{M},$$

$$K_4 = K_3 / r. \quad (3d)$$

$M = m_s / m_\pi$  where  $m_s$  is the source mass for which the potential is computed,  $m_\pi = 139.57 \text{ MeV}/c^2$  (the mass of the pi-meson). The  $m_t$  is the responding test mass, and  $m_{Gp} = 1.72 \times 10^{-22} \text{ MeV}/c^2$  (the hypothesized “smallest” particle). The calculation units are: masses in  $\text{MeV}/c^2$ ,  $r$  in fermis, and  $V_U$  in  $\text{MeV}$ . The macro-scale conversion to these units are:  $1.7826915 \times 10^{-33} \text{ MeV}/c^2$  per kg;  $10^{15} \text{ fm/m}$ ;  $1.496 \times 10^{11} \text{ m/AU}$ ;  $1.6022 \times 10^{-13} \text{ J/MeV}$ ; and  $63240 \text{ AU/lyr}$ ;  $1 \text{ SU} = 1.99 \times 10^{30} \text{ kg}$ .

$T(r, \sqrt{M})$  becomes imaginary when  $M$  is negative because of the  $\sqrt{M}$  factor in (3d), giving  $V_U$  an imaginary component. This is not true of  $V_N$  which is always real, retaining the same function but changing sign. We assume an absolute value for  $M$  in  $E_0$  and  $E_1$ . This guarantees  $V_U$  decays at large distances when  $M < 0$ .

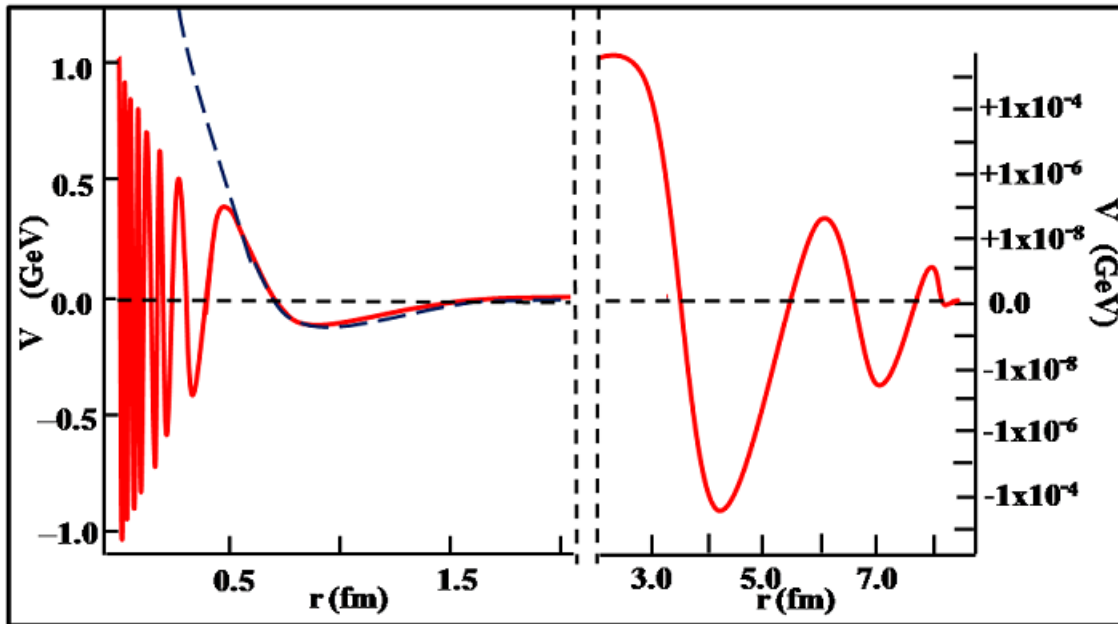


**Figure 1.** Shown is the characteristic behavior at the quantum scale. The solid red line is  $V_U$  and the broken blue line is  $V_{Y-mod}$ . There are no values for  $V_{Y-mod}$  in the lower (smaller  $r$ , near-field) or upper (larger  $r$ , far-field) tail regions. The  $r$ -values between  $\sim 0.5$  and  $2.0$  are the usual values for  $V_{Y-mod}$  for the pi-meson interaction ranges. The  $V_U$ 's near-field oscillation ( $r < 0.25$ ) approaches its maximum amplitude ( $\pm 1.234$  GeV) where  $V_{Y-mod}$  increases exponentially. The  $V_U$ 's damped oscillation in the far-field ( $r > 2.5$ ) is shown on an exaggerated scale. ( $m_s = m_t = m_\pi$ ).

### 3.1. Quantum-Scale Behavior of $V_U$

At quantum scales, the dominating terms in  $V_U$  are the  $K_1$  (3c), and  $K_3$  and  $K_4$  (3d). As the  $r$  increases, the  $K_1$  and  $K_4$  terms reverse rolls in their dominance.  $V_U$  exhibits the same behavior for all quantum-scale source masses down to the smallest possible mass.

The pi-meson (Figure 1) is a typical example of the characteristic behavior of  $V_U$  at the quantum scale down to the smallest possible masses. Values for the neutron-neutron interaction with pi-meson exchange,  $V_{Y-mod}$ , were taken graphically from Figure 3.3 [28]. In this region,  $V_U$  agrees reasonably well with  $V_{Y-mod}$  in shape and amplitude (RMS  $\sim 20\%$ , mean  $\sim 2\%$ ) for the usual range for the pi-meson interactions ( $\sim 0.3$  fm to  $\sim 2.5$  fm). Although the central region agrees, the tails have different behavior. In the near-field region,  $V_U$  oscillates as  $r$  decreases ( $r < \sim 0.5$  fm), asymptotically approaching a maximum of  $\sim 1.234$  GeV.  $V_{Y-mod}$ , however, appears to exponentially grow without oscillation (but, the function is not considered valid below  $\sim 0.3$  fm). In the far-field region, both  $V_{Y-mod}$  and  $V_U$  damp exponentially as  $r$  increases, approaching zero as  $r \rightarrow \sim 10$  fm. However,  $V_U$  oscillates, while  $V_{Y-mod}$  appears to monotonically approach zero. At the limits of measurement ability in this region, both  $V_U$  and  $V_{Y-mod}$  would appear approximately the same.



Qualitatively, the oscillation of  $V_U$  serves the same purpose as it does for  $V_{Y-mod}$ . There, the region of changing slope indicates adjacent areas of repulsion and attraction that keep the quarks inside a proton, not-too-far but not-too-close to each other, thus maintaining a stable particle configuration. It is the ever increasing frequency of oscillation of  $V_U$  at the smallest particle interactions that provide a mechanism to shield the particles and prevent them from collapsing into each other. Also, it keeps the near-field potential from growing without bound, thus, protecting the integrity of the space-time fabric. The damped oscillation of  $V_U$  at larger  $r$  provides the basis of the transition to the  $1/r$  behavior at macro-scale distances.

### 3.2. Macro-Scale Behavior of $V_U$

The macro behavior of gravity is a very wide-ranged effect, covering everything from the ordinary scales of every-day life to the largest cosmic scales. At macro scales, the dominating terms in  $V_U$  are the  $K_2$  (3d) and  $K_f$  (3c), and the characteristic behavior is the same at all macro scales whether the source mass is small (ordinary scales) or cosmic in magnitude.

Figure 2 shows an example of the characteristic behavior at ordinary scales, for separations from thousands of meters down to the transition to quantum scales. In this range,  $V_U$  is equal to  $V_N$  before it begins oscillating. The horizontal axis plots the natural log ( $\ln$ ) of  $r$  because of the wide range covered ( $3 \times 10^{-7}$  m to  $9 \times 10^3$  m). Similarly, the vertical axis is plotted on a log scale where the potential (in Joules) is divided by the Newton's gravitational constant  $G$ . Since the logarithm function is not valid for negative arguments, the absolute value of the argument was plotted with the sign of the potential. In the log-log format the  $1/r$  behavior becomes a straight line, so  $\ln(|V_N|/G)$  takes on positive values for  $V_N < G$ , but a negative value for  $V_N > G$ .

For  $r > \sim 0.001$  m ( $\ln(r) \sim 7$ ) with the masses shown,  $V_U$  is an attractive potential that agrees with  $V_N$  (to within the uncertainty in  $V_N$ ,  $\pm 0.00135\%$ ). At sub-millimeter ranges ( $\ln(r) < -7$ ), as  $r$  decreases,  $V_U$  begins to diverge from  $V_N$ . The break-point shifts to shorter ranges with decreasing mass (roughly as  $\Delta \ln(m) / \Delta \ln(r) \simeq 2$ ). It is at this point that a transition from ordinary  $1/r$  macro-scale behavior begins to take place, and  $V_U$  begins to oscillate. This oscillating transition (beginning at the first oscillation peak) is evident even at the larger cosmic scales.

Figure 3 shows a detail of the transition to oscillation for the 55 kg case. The oscillatory behavior is similar to what was seen in the quantum case. Here, the maximum amplitude in the oscillation is reached almost immediately, differing slightly from the quantum case which builds to its maximum more slowly. As the mass and range combination approach the quantum case, the transition region evolves into the maximum limits seen in the quantum-scale behavior.

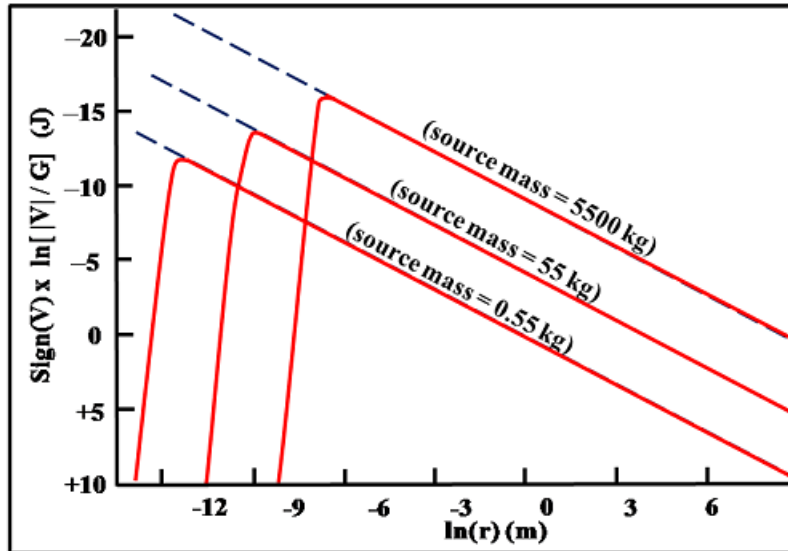


**Figure 2.** Shown is the characteristic behavior at ordinary macro scales. The solid red line is  $V_U$  and the broken blue line is  $V_N$ . There is exact agreement between  $V_U$  and  $V_N$  before  $V_U$  begins oscillation (between attractive and repulsive behavior) in its transition to the quantum scales. Both are attractive potentials to that point. ( $G = 6.67432 \times 10^{-11}$ ,  $m_t = 1$  kg).

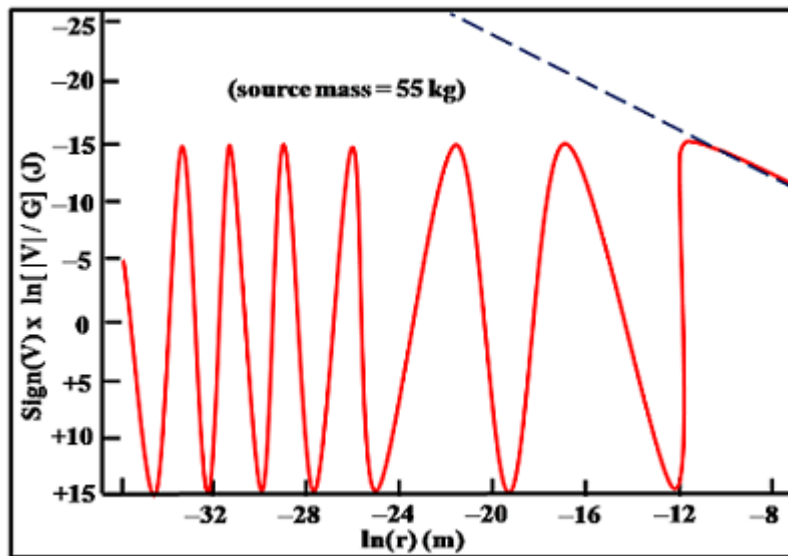


**Figure 3.** This shows a detail of the comparison of the  $V_U$  and  $V_N$  in the transition region between macro scales down to quantum scales for the 55 kg source mass. The solid red line is  $V_U$  and the broken blue line is  $V_N$ . ( $G = 6.67432 \times 10^{-11}$ ,  $m_t = 1$  kg).

We draw another analogy between the macro and quantum cases regarding the effective purpose of the oscillation. The quantum case provides particle stability and a protection for the integrity of the fabric of space. We hypothesize here that, for the macro case, the oscillation transition keeps objects from breaking the surface barrier of solid objects. This, in effect, prevents them from tunneling into one another while, at the same time, allowing them to be in apparent contact.

Even though  $V_N$  and  $V_{Y-mod}$  both have some  $1/r$ -like behavior, the connection between gravity and quantum mechanics has not yet been definitively established. We propose that  $V_U$ 's oscillating transition represents this connection, and is seen in the Casimir force.

The Casimir force was first proposed in the 1940's by Hendrik Casimir [29], and is identified as a quantum mechanical effect, resulting from "zero-point electromagnetic fluctuations". In the very tiny space between the two plates, virtual electrons pop into and out of existence at times too short to be measured. This constantly fluctuating charge and mass in the space gives rise to a weak force that is not related to any currents that might be induced in the two plates. Usually, the weak force is attractive. But a weaker repulsive force has also been observed in the nanometer range [30, 31], and Asorey et al. have analyzed the boundary conditions for the attractive-repulsive nature of the effect [32]. It is this range where  $V_U$  sees the oscillating transition in its potential.

The example of  $V_U$ , at cosmic scales is seen in Figure 4. With a source mass equal to our sun,  $m_s = 1$  SU,  $V_U$  agrees with  $V_N$  (plus the GR correction) to  $<0.001\%$  over the planetary orbit ranges. The departure of  $V_U$  from  $V_N$  occurs well within the orbit of Mercury with the oscillation beginning outside the Sun's surface (if you could get close enough, you would feel the adjacent repulsive and attractive regions in the potential before actually crossing to the Sun's interior).

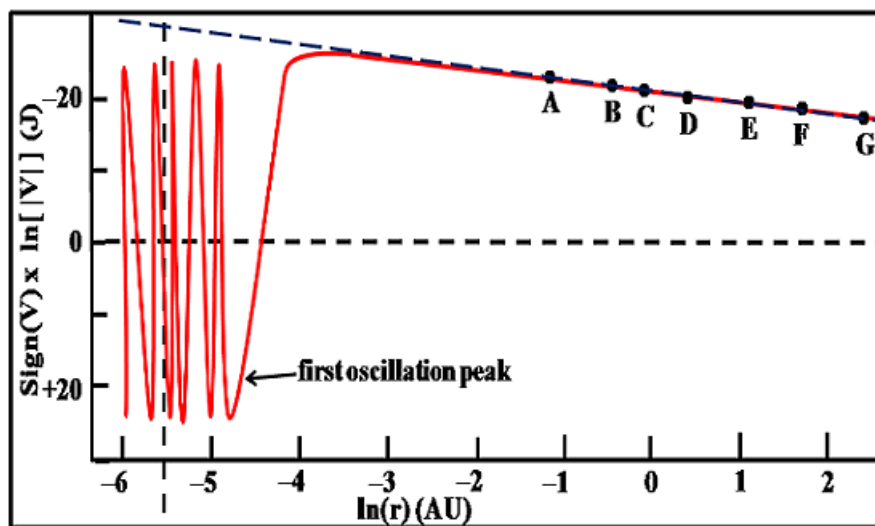


**Figure 4.** Shown is the characteristic behavior at cosmic (solar system) scales. The solid red line is  $V_U$  and the broken blue line is  $V_N$ .  $V_U$  and  $V_N$  agree perfectly at the typical planetary distances.  $V_U$  diverges from  $V_N$  as it begins its oscillation phase well inside the orbit of Mercury (A). The vertical broken black line at  $r = 0.0047$  AU indicates the Sun's radius. The bullets indicate the planetary orbits: A = Mercury at 0.387 AU; B = Venus at 0.723 AU; C = Earth at 1.0 AU; D = Mars at 1.524 AU; E = Asteroid Ceres at 2.77 AU; F = Jupiter at 5.203 AU; G = Saturn at 9.359 AU. ( $m_s = 1$  SU, and  $m_t = 1$  kg).

It should be noted for the sake of purity that the straight-forward application of Newton's law assumes a point source relative to the test mass. In reality, the Sun is actually an extended source compared to the size and distance of Mercury. The source mass in this comparison is assumed to be concentrated within a sufficiently small space relative to the orbit locations on the plot. This is true for most of the planets.

Oscillatory behavior in  $V_U$  is evident even for the largest masses, beginning "at the surface" and continuing for some distance. The transition from oscillation to  $1/r$  is the point referred to here as the "first oscillation peak". Table 1 shows the first oscillation peak for several cosmic bodies. The neutron star and the black hole, here, are representative examples. For a typical not-too-massive black hole,  $V_U$  does not take on the  $1/r$  form of Newton until well outside the black hole's event horizon ( $\sim 15 \times 10^6$  m).

**Table 1.** Shown are examples of the range for the first oscillation peak as  $r$  decreases. Our Solar System is  $\sim 2 \times 10^9$  AU from the center of our Milky Way galaxy – outside of the expected oscillation region for the Galaxy's potential assuming most of the mass is in the central core.

Source Body	Mass (SU)	Radius (AU)	First Oscillation Peak (AU)
Neutron star	$3 \times 10^{-5}$	$\sim 1.08 \times 10^{-7}$	$3 \times 10^{-5}$
Black Hole (BH)	$1.5 \times 10^{-4}$	$\sim 3.2 \times 10^{-8}$	$9 \times 10^{-5}$
Sun	1.0	0.0047	$\sim 0.0093$
SgrA-*BH	$\sim 4 \times 10^6$	1	253
Milky Way Galaxy	$\sim 6 \times 10^{11}$	$\sim 2 \times 10^{10}$	$6 \times 10^5$

This oscillation in the potential could be interpreted as the source of the quantum-like behavior predicted in the space surrounding the black hole [33].

We take our Milky Way Galaxy as an example of a larger cosmic scale. It is classified as a spiral galaxy, with a central core (a bar-shaped bulge), surrounded by a flattened disk, and enclosed by several spiral rings. The roughly elliptically-shaped rings are higher density bands of dust and stars separated by relatively dust-free regions, but, the ring-area contains negligible mass relative to the bulge and disk. The Galaxy's mass includes this inner region ( $6 \times 10^{10}$  SU, 8 kps  $\simeq 2 \times 10^8$  AU) plus a surrounding spherical halo of dark (non-visible) matter that has the gravitational effect of additional mass.

The Galaxy is believed to have a super-massive black hole at its center (SgrA-\*, Sagittarius A-star). It is about the mass of 4 million Suns, and  $\sim 200$  times the size of our Sun.  $V_U$  indicates an oscillation

in its potential that extends as far as 253 AU (about six times the distance of Pluto to the Sun). The first oscillation peak is outside SgrA-\*'s event horizon, but within the more extended central Galaxy bulge.

Assuming the bulk of the Galaxy's mass is contained within a relatively small region of the core,  $V_U$  indicates that its first oscillation peak occurs at  $\sim 6 \times 10^5$  AU. The potential converges to Newton's  $1/r$  decay by  $\sim 2 \times 10^8$  AU (1 kilo parsec), still within the Galaxy's core region. To our nearest neighbor, SgrDEG (Sagittarius Dwarf Elliptical Galaxy), at  $\sim 5 \times 10^9$  AU ( $\sim 25$  kpc), the Galaxy's potential would be the expected  $1/r$  attraction as predicted by Newton.

A primary tool in determining the Galaxy's mass distribution is its "rotation curve" which indicates the rotation speed of stars at any radial distance. The radial velocity is determined by balancing gravity (generally based on the monotonically decreasing potential of Newton) with the centrifugal force. This produces a smooth curve with a large bump around the core region where rotation speed is fastest, and then settles to a flat tail in the outer regions [34]. Matter-density shock waves and kinematic interactions with orbiting satellite galaxies provide much of the explanation for the observed structure [35, 36].

Sofue [37] notes that the calculated rotation curve agrees well with the observed data except for the wavy, small-scale variations in the observed curve which cannot be attributed to the basic mass distribution, and may indicate some other underlying structure. There is a possibility that matter-density waves generated within the  $V_U$  oscillating region might offer additional information about the wavy behavior seen in the rotation curve. This requires further study.

An additional cosmological effect that  $V_U$  might address is the recent discovery of multiple, well-defined concentric rings in the proto-planetary disks around young *Kepler* stars [38, 39]. Models of planetary formation [40] include effects such as, gravitational interactions between embryo-planets, collisions forcing bodies into trapped resonances, and dust trapping in radial pressure bumps. Results around the *Kepler* stars detected disk behavior as close as Mercury is to our Sun, and as far out as Jupiter and beyond, but without the detection of planetary bodies. The stars were considered too young for the observed ring formation, and it was suggested that a collision-based disk-sculpting mechanism might explain the effects. The possibility that events generated within the  $V_U$  oscillating region might contribute to early ring formation, and, requires further study.

## 4. Conclusions

This initial effort produced a universal potential characterizing both the smallest quantum scales through the macro (and cosmic) scales. As developed, it was not intended to model specific mechanisms, simply an operational characterization of the field behavior in general.  $V_U$  reproduces the oscillatory behavior characteristic of particle confinement at quantum scales, and the  $1/r$  behavior of macro scales.

It also demonstrates a transition between the two regions that occurs at approximately the same region as the Casimir effect. (This could imply that the Casimir effect is a true transition between the macro and quantum scales). The  $V_U$  is the potential that was developed for the FRACEP model described in [17].

Oscillatory behavior also shows up at the cosmic scales. The small radius with a large mass produces oscillations that could be interpreted as quantum effects at cosmic scales, as expected around black holes. Such effects are not predicted by Newtonian gravity or GR – they require quantum gravity models. Further, the oscillation region might offer some additional insight into the structural detail observed in both galactic and planetary system formation.

The data for the analysis was based on the traditional understanding of the nature of matter, that is, all mass is positive. We show that the characterization of negative mass evolves naturally from the function required to satisfy both the quantum and the macro-gravity scales in the form of terms with the square-root of the source mass. These terms provide an imaginary component to the potential when the mass becomes negative, implying behavior that is not totally symmetric between the positive-mass source and the negative-mass source. This asymmetry might offer some insight into the nature and behavior of dark matter and dark energy generally accepted as present in the universe.

## References

- [1] M.S. Turner, Dark Matter: Theoretical Perspectives. *Proc. Nat. Acad. Sci. USA* 90 (**1993**): 4827.
- [2] B.A. Dobrescu and D. Lincoln, Mystery of the Cosmos. *Sci. Am.*, July (**2015**): 32-39.
- [3] J.P. Ostriker and P. Steinhardt, New Light on Dark Matter. *Science*, 300 (**2003**): 1909-1913.
- [4] A. Cho, Crunch Time for Dark Matter Hunt. *Science*, 351 (**2016**): 1376-1377.
- [5] L. Poffenberger, Diversifying the Dark Matter Portfolio. *APS News* 27 (**2018**): 1.
- [6] L.I. Schiff, Dirac's Equation for a Central Field. In *Quantum Mechanics*; McGraw-Hill: New York, USA, **1949**.
- [7] L.I. Schiff, Gravitational Properties of Antimatter. *Proc. Nat. Academy of Sci.*, 45 (**1959**): 60-80.
- [8] S. Weinberg, "Space Inversion and Time-Reversal". In *The Quantum Theory of Fields, vol. 1*; Cambridge Univ. Press: Cambridge, UK, **2005**.
- [9] I. Newton, Rules for the Study of Natural Philosophy. In *The Principia, Book 3*, trans. B. Cohn and A. Whitmann; U. California Press: Berkley, USA, **1999**.
- [10] M. Jammer, The Gravitational Concept of Mass. In *Concepts of Mass in Classical and Modern Physics (Reproduction of 1961 Harvard Univ. Press Edition)*; Dover Pub. Inc.: Mineola, NY, **1997**.
- [11] H. Bondi, Negative Mass in General Relativity. *Rev. Mod. Phys.*, 29 (**1957**): 423-428.

*Int. J. Modern Theo. Physics*, **2019**, 8(1): 1-16

- [12] W.B. Bonner, Negative Mass in General Relativity. *Gen. Rel. and Grav.*, 21 (**1989**): 1143-1157.
- [13] F. Hoyle, G. Burbidge, and J.V. Narlikai, A Different Approach to Cosmology, *Phys. Today*, April, 38 (**1999**): 38-44.
- [14] F. Hoyle, G. Burbidge, and J.V. Narlikai, *A Different Approach to Cosmology*; Cambridge U. Press: Cambridge, UK, **2000**.
- [15] Yi-Fang Chang, Field Equations of Repulsion Force between Positive-Negative Matter, Inflation Cosmos and Many Worlds. *Int. J. Mod. Theoretical Phys.*, 2 (**2013**): 100-117.
- [16] J.P. Petit and G. D'Agostini, Cosmological Bimetric Model with Interacting Positive and Negative Masses and Two Different Speeds of Light, in Agreement with the Observed Acceleration of the Universe. *Mod. Phys. Lett. A*, 29(**2014**): 1450182 (15 pages).
- [17] J.A. Giannini, Fractal Rings and Composite Elementary Particle (FRACEP) Model: A Picture of Composite Standard Model Fundamental Particles. *Bull. Am. Phys. Soc.*, 61 (6) (**2016**), Session T1.031.
- [18] Simone Giani, On Velocities Beyond the Speed of Light C. *CERN*, *arXiv:hep-ph/9712265v3* (**2008**): 1-11.
- [19] Simone Giani, Experimental Evidence of Superluminal Velocities in Astrophysics and Proposed Experiments. *AIP Conf. Proc.*, 458 (**2008**): 881-888.
- [20] G. Cacciapaglia, A. Deandrea and L. Panizzi, Superluminal Neutrinos in Long Baseline Experiments and SN1987A. *J. High Energy Physics - Springer*, *JHEP* 11 (**2011**): 137 (22 pp).
- [21] R. Takahashi and H. Asada, Observational Upper Bound on the Cosmic Abundances of Negative-Mass Compact Objects and Ellis Wormholes from SLOAN Digital Sky Survey Quasar Lens Search. *Astr. J. Lett.*, 768 (**2013**): L16 (4pp).
- [22] S. Mbarek and M.B. Paranjape, Negative Mass Bubbles in de Sitter space-time. *Phys. Rev.*, D90 (**2014**): 101502(R).
- [23] M.A. Khamehchi, K. Hossain, M.E. Mossman, Y. Zhang, Th. Busch, M. McNeil Forbes and P. Engels, Negative-Mass Hydrodynamics in a Spin-Orbit-Coupled Bose-Einstein Condensate. *Phys. Rev. Lett.*, 118 (**2017**): 155301.
- [24] The ALPHA Collaboration and A.E. Charman, Description and First Application of a New Technique to Measure the Gravitational Mass of Antihydrogen. *Nature Comm.*, 4 (**2013**): 1785 (8pp).
- [25] M. Ahmadi, *et al.*, Observation of the 1S-2P Lyman- $\alpha$  Transition in Anti-hydrogen. *Nature* 561 (**2018**): 211-217.
- [26] B. Schwarzschild, Theorists and Experimenters Seek to Learn Why Gravity Is So Weak. *Physics Today*, September, 22 (**2000**): 22-24.

*Int. J. Modern Theo. Physics*, **2019**, 8(1): 1-16

- [27] V.M. Blanco and S.W. McCuskey, *Basic Physics of the Solar System*; Addison-Wesley Publishing Company, Inc; Reading, MA, USA, **1961**: 216-219.
- [28] C.A. Bertulani, Nucleon-Nucleon Interactions. In *Nuclear Physics in a Nutshell*; Princeton U. Press; Princeton, NJ, USA, **2007**: 71-95.
- [29] H.B.G. Casimir, D. Polder, The Influence of Radiation on the London-Van der Waals Forces. *Phys. Rev.*, 73 (**1948**): 360-372.
- [30] J. Miller, Casimir Forces Between Solids Can Be Repulsive. *Physics Today*, February (**2009**):19-22.
- [31] J.N. Munday, F. Capasso and V.A. Parsegian, Measured Long-Range Repulsive Casimir-Lifshitz Forces. *Nature*, 457 (**2009**): 170-173.
- [32] M. Asorey and J.M. Munoz-Costaneda, Attractive or Repulsive Casimir Effect and Boundary Condition. *Nanosystems: Phys., Chem., Math.*, 2 (4) (**2011**): 20-31.
- [33] G. Dvali, Quantum Black Holes. *Physics Today*, January (**2015**): 38-43.
- [34] O.Y. Gnedin, W.R. Brown, M.J. Geller and S.J. Kenyon, The Mass Profile of the Galaxy to 80 KPC. *Astro. J Lett.*, 720 (**2010**): L108 (5pp).
- [35] W.W. Roberts and W.B. Burton, The Large-scale distribution of Interstellar Matter in the Context of Density-Wave Theory. In *Topics in Interstellar Matter; Commission 34 Session, General Assembly, 16<sup>th</sup>, Grenoble, France, August 25, 1976*; Dordrecht D. Reidel Publishing Co., **1977**: 195-205.
- [36] R.A. Benjamin, and H. Beuther, H. Ling and T. Hennig, eds., The Spacial Structure of the Galaxy: Something Old, Something New .... In *Massive Star Formation: Observations Confront Theory, ASP Conference Series*, 387 (**2008**): 275-380.
- [37] Y. Sofue, M. Honma, T. Omodaka, Unified Rotation Curve of the Galaxy – Decomposition into de Vaucouleurs Bulge, Disk, Dark Halo, and the 9-kpc Rotation Dip. *Publ. Astr. Soc. Japan*, 61 (**2009**): 227-236.
- [38] C.P. Dullemond, *et al.*, The Disk Sub-structures at High Angular Resolution Project (DSHARP). VI. Dust Trapping in Thin-ringed Protoplanetary. *Astro. J Lett.*, 869 (**2018**): L46 (21pp).
- [39] R.S. Sobrinho, *et al.*, Debris Disks among *Kepler* Solar Rotational Analog Stars. *Astro. J Lett.*, 869 (**2018**): L40 (9pp.).
- [40] Y. Alibert, *et al.*, Theoretical Models of Planetary System Formation: Mass vs. Semi-major Axis. *Astronomy and Astrophysics*, 558 (**2013**): A109 (13pp).